HOT-ELECTRON DETECTORS: TOWARD RECORD SENSITIVITY VIA DISORDER-SUPPRESSED ELECTRON-PHONON COUPLING

M. E. Gershenson, D. Gong, and T. Sato
Department of Physics and Astronomy, Rutgers University, Piscataway, NJ 08854

B. S. Karasik and W. R. McGrath
Jet Propulsion Laboratory, California Institute of Technology, Pasadena, CA 91109

A. V. Sergeev
Dept. of Electrical and Computer Engineering, Wayne State University, Detroit, MI 48202

Recently we proposed a concept of a submm/FIR direct detector based on electron heating in superconducting microbridges at ultra-low temperatures [1]. The main advantages of the hot-electron direct detectors (HEDDs) are an unparalleled sensitivity, simplicity of fabrication, and large-array scalability. Basic parameters of the HEDDs, the time constant and sensitivity, are determined by the electron-phonon relaxation time, $\tau_{e\text{-}ph}$. The strong temperature dependence of the electron-phonon coupling and effects of disorder allow to suppress the electron-phonon interaction and to enhance electron heating by electromagnetic radiation. As the first step toward implementation of the HEDDs, we have measured $\tau_{e\text{-}ph}$ at $T = 0.04$ - 1 K in disordered hafnium films with $T_c = 0.3$-0.5 K. Below $T \approx 0.5$ K, we observed the dependence $\tau_{e\text{-}ph}(T) = 6.5\times10^{-8}\ (T/1\text{K})^{-4}$ s, which is in a very good agreement with the theory of electron-phonon interactions in disordered conductors. Slow electron-phonon relaxation with $\tau_{e\text{-}ph}$ as large as 25 ms at $T = 0.04$ K results in a record sensitivity. Scaling of the in-plane sensor dimensions down to ~ 1 μm would result in the noise equivalent power $NEP \approx 10^{-20}$ W/Hz$^{1/2}$ at $T = 0.1$ K, which is two orders of magnitude better than that for the state-of-the-art bolometers.

Introduction

Future far infrared (FIR) radioastronomy missions (SPIRIT, the 10m FIR telescope, and SPECS) will require significant improvement in the sensitivity of radiation detectors in the 40-500 μm wavelength range, and integration of the detectors in large arrays for sky mapping applications [2]. The photon-limited noise equivalent power (*NEP*) of a detector combined with a cooled space telescope is expected to be better than 10^{-19} W/√Hz [3], or even lower for narrow band applications. The state-of-the-art bolometers currently offer $NEP \sim 10^{-17}$ W/√Hz at 0.1 K, along with the time constant $\tau \sim 10^{-3}$ s [4,5]. High sensitivity of these bolometers is achieved by using the so-called spiderweb suspension. For higher sensitivity, thermal conductance between the device and the heat sink should be further reduced. However, this will slow down the bolometer

response and enhance the 1/f-noise. Better detectors will be required to meet the needs of the upcoming space missions.

Recently, we proposed a new approach to the sensitivity improvement, based on implementation of electron heating in superconducting microbridges at sub-Kelvin temperatures [1]. The innovative idea is to use a superconducting hot-electron detector with electron-phonon inelastic scattering time $\tau_{e\text{-}ph}$ controllably adjusted to the required time constant, τ. Wide-range variation and precise control of the electron-phonon scattering rate is possible due to a strong temperature dependence of $\tau_{e\text{-}ph}$; further increase of $\tau_{e\text{-}ph}$ might be possible by controllably introduced disorder (electron scattering from boundaries, impurities, and defects). The exceptionally high sensitivity of the HEDDs can be achieved due to a very small heat capacity of electrons in a micron-size sensor. We expect that an antenna- or waveguide-coupled micron-size HEDD with a small time constant $\tau \sim 10^{-3} \div 10^{-5}$ s will exhibit at $T = 0.1\text{-}0.3$ K the photon-noise-limited performance in millimeter, sub-millimeter, and infrared wavelengths [6]. Besides this record sensitivity, the hot-electron detectors will have other attractive features. They can be fabricated on a bulk substrate and integrated into arrays, their impedance can be easily matched with the planar antenna's impedance.

Concept of the ultra-low-temperature HEDD

Operation of both conventional and hot-electron detectors can be illustrated by Fig. 1. The radiation is absorbed by electrons in a thin-film sensor. The electron-phonon coupling in the sensor is characterized by the electron-phonon thermal conductance $G_{e\text{-}ph} = C_e/\tau_{e\text{-}ph}$, where $C_e = \gamma T$ is the electron heat capacity and γ is the Sommerfeld constant. Escape of non-equilibrium phonons into the heat bath is described by the escape time τ_{es} and the thermal conductance $G = C_{ph}/\tau_{es}$, where C_{ph} is the heat capacity of phonons in the combination thin-film sensor + substrate. High sensitivity of conventional bolometers is due to a significantly reduced coupling to the heat bath ($G << G_{e\text{-}ph}$). The noise equivalent power of an optimally designed bolometer is limited by thermodynamic fluctuations of the temperature in the process of the heat transfer to the heat bath:

$$NEP = \sqrt{4k_B T^2 G}\,. \qquad (1)$$

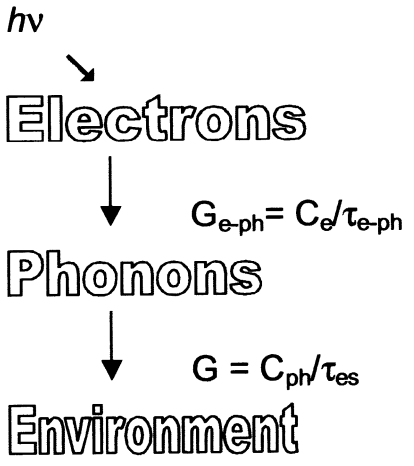

Fig. 1. Scheme of operation for bolometers and hot-electron detectors.

On the other hand, in a hot-electron detector, a weak electron-phonon coupling serves as the bottleneck of the energy transfer between electrons and the environment ($G_{e\text{-}ph} << G$). This requirement can be easily satisfied at ultra-low temperatures, because G is typically proportional to T^3 [7], whereas $G_{e\text{-}ph}$ decreases much faster with lowering

T, usually as $T^{(4\div5)}$. Reducing the film thickness also helps to satisfy the condition $G_{e\text{-}ph} << G$, because G, unlike $G_{e\text{-}ph}$, is inversely proportional to the film thickness [8]. In this hot-electron regime, the radiation overheats the electrons in a superconducting film, while phonons in the film play the role of a heat sink for electrons (for a review, see [9]). The HEDD time constant coincides with the electron-phonon scattering time $\tau_{e\text{-}ph}$. For a HEDD with the sensitivity limited by fluctuations of the electron temperature,

$$NEP = \sqrt{4k_B T^3 \gamma V / \tau_{e-ph}} \ , \qquad (2)$$

where V is the sensor volume. Comparison between (1) and (2) shows that for the same time constant τ and in-plane dimensions of a sensor, hot-electron detectors offer an ultimate sensitivity [8]. This difference can be further increased, since it is feasible to reduce in-plane dimensions of the hot-electron sensor down to ~ 1 μm, a very difficult task for a conventional bolometer. Another attractive feature of the HEDDs is that they can be fabricated on a conventional substrate, because the thermal conductivity G is irrelevant.

The schematic design of a micron-size HEDD is shown in Fig. 2. To maximize the electron heating at sub-Kelvin temperatures, a special design of the current leads is required. The leads should be fabricated from a superconductor with a superconducting energy gap Δ much larger than that of the sensor, e.g., Nb. The dc bias and rf currents will flow freely through the structure, whereas outdiffusion of hot electrons with energies $\varepsilon < \Delta$ will be blocked by Andreev reflection [10].

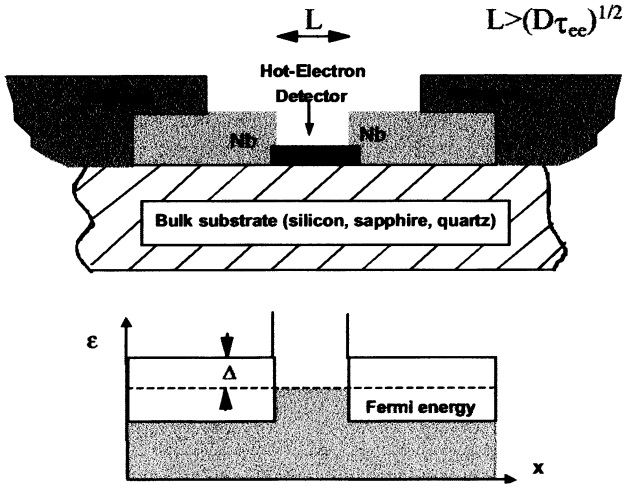

Fig. 2. The schematic design of a hot-electron detector. The sensor is flanked by superconducting current leads ("Andreev mirrors"), which prevent outdiffusion of hot electrons. The energy gap in the sensor is suppressed either by the temperature $T \sim T_c$ or by a weak magnetic field at $T<T_c$. This magnetic field does not affect the gap in the leads since H_{c2}(leads) >> H_{c2}(sensor). The total length of superconducting leads should be small to reduce *rf* losses at high frequencies. The antenna is fabricated from a high-conductivity normal metal (Au).

The lower limit on the sensor length, L, is imposed by the proximity effect: L should be larger than the coherence length in a normal metal, $L_T = (\hbar D/2\pi k_B T)^{1/2}$, to preserve difference between the critical temperatures of the sensor and superconducting leads. Thus, for a disordered film with the diffusion constant $D \sim 1$ cm^2/s, L should be much larger than $2L_T \sim 0.1$ μm at $T = 0.1$ K. Typically, this requirement is also sufficient to ensure high quantum efficiency of the HEDD at frequencies $f > \Delta/h$ (e.g., for *Nb* leads, Δ/h corresponds to 360 GHz). Indeed, for high quantum efficiency, the electrons, which are the current carriers in

superconductors at high frequencies $f > \Delta/h$, must be thermalized within the HEDD due to electron-electron interactions. The electron-electron inelastic scattering time $\tau_{e\text{-}e}$ is by many orders of magnitude smaller than $\tau_{e\text{-}ph}$ in disordered thin films at low temperatures [8]. For electron thermalization, the length L should be larger than the diffusion length of electrons with energies $\varepsilon \sim \Delta$, $L_{e\text{-}e} = [D\tau_{e\text{-}e}(\Delta)]^{1/2}$. The two scales, L_T and $L_{e\text{-}e}$, are of the same order of magnitude in ultra-thin disordered films at $T < 1$ K. Thus, the sensor length ~ 1 μm should be sufficient to minimize the proximity effect and to ensure electron thermalization.

Electron-phonon scattering at sub-Kelvin temperatures.

As the first step toward development of ultra-sensitive HEDDs, it is necessary to verify if an ultra-long electron cooling time $\tau_{e\text{-}ph} \sim 10^{-3}$ s can be realized within the temperature range $T = 0.05$-0.3 K, accessible by modern flight qualified refrigerators. We have measured $\tau_{e\text{-}ph}$ in thin films of hafnium deposited on sapphire substrates. Hafnium is a promising material for ultra-low-temperature HEDDs ($T_c = 0.13$K for bulk Hf). In these preliminary experiments, instead of using superconducting leads to block outdiffusion of hot electrons, we fabricated a very long meander-type structure with the total length $L >> \sqrt{D\tau_{e-ph}}$ (Fig. 3). The critical temperature and resistivity of magnetron-sputtered Hf films depend strongly on the argon pressure and deposition rate. By optimizing the deposition parameters, we were able to increase T_c up to 0.5 K. The superconducting transition and the temperature dependence of the critical magnetic field H_{c2} for one of the samples is shown in Fig. 4. The thickness of Hf films was varied between 250 Å and 850 Å to keep the sheet resistance R in the 30-50 Ω range (for better impedance matching of the antenna-coupled HEDDs).

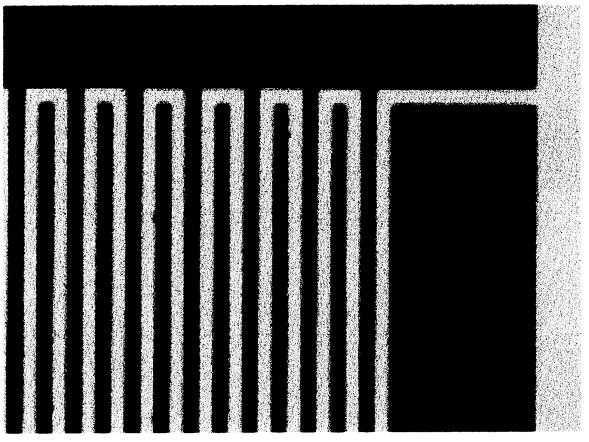

Fig. 3. Microphotograph of a portion of the meander-type Hf structure on a sapphire substrate. The width of the strip is 5 μm, the total length is 10 cm, the total area occupied by the meander is 1×1 mm^2.

In the heating experiments, the resistance of a sample has been measured at a small ac current I_{ac} by a resistance bridge as a function of the temperature and the heating dc current I_{dc}. The temperature dependence of quantum corrections to the resistance has been used as an electron "thermometer" in the temperature range $T > T_c$. Below T_c, the sample was driven into the resistive state by applying the magnetic field. The resistive state is very sensitive to electron overheating; this allows measuring $\tau_{e\text{-}ph}$ with an unparalleled accuracy.

The experimental procedure of finding the thermal conductivity between electrons and phonons, $G_{e\text{-}ph}$, is illustrated in

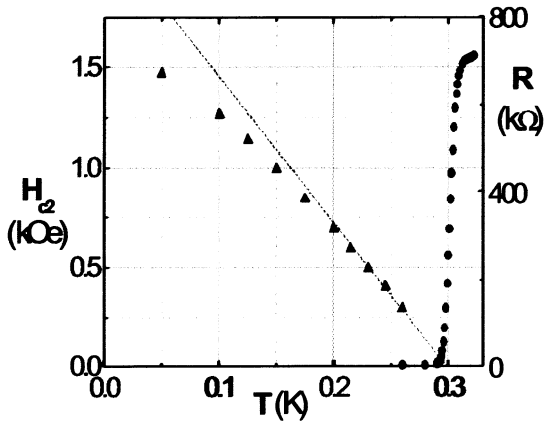

Fig. 4. The superconducting transition $R(T)$ at $H = 0$ with $\Delta T_c = 7$mK (dots) and the temperature dependence of the upper critical field H_{c2} (triangles) for a Hf meander structure with d = 250 Å and R =38 Ω.

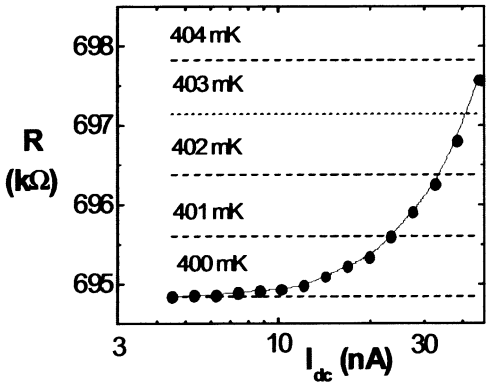

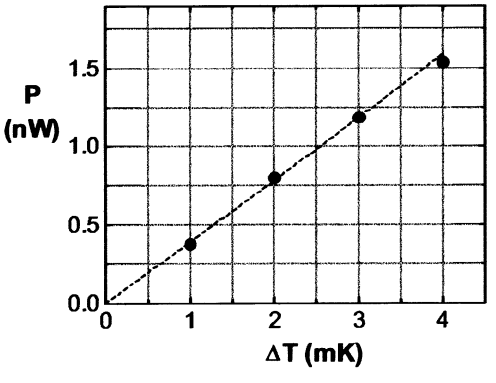

Fig. 5. For small electron overheating, the thermal conductivity between electrons and phonons can be found from the heat balance equation

$$\frac{P}{V} = G_{e-ph}\Delta T = \frac{C_e}{\tau_{e-ph}(T)}\Delta T \quad , (3)$$

where $P = I_{dc}^2 R$ is the Joule power dissipated in a thin film of volume V, and $\Delta T = T_{el} - T_{ph}$.

The temperature dependences $G_{e\text{-}ph}(T)$ measured for samples with different T_c are shown in Fig. 6. By assuming that the electron heat capacity in Hf films is the same as in bulk Hf [$\gamma = 160$ W/(m^{3}K^2)], we can estimate the temperature dependence of the electron cooling time $\tau_{e\text{-}ph}$ in these films (Fig. 7).

We compare the experimental data with the theoretical estimate of the electron cooling time in the "dirty" limit ($q_T l << 1$, where q_T is the

Fig. 5. Heating measurements at $T = 0.4$ K and $B = 960$ G for a sample with $T_c = 0.48$ K. Top panel: the difference between the electron and phonon temperatures, ΔT, is obtained from comparison of the zero-dc-bias $R(T)$ (dashed horizontal lines) with the dependence $R(I_{dc})$ measured at a fixed $T = 0.4$ K (solid dots). Bottom panel: the thermal conductivity between electrons and phonons $G_{e\text{-}ph}$ is a coefficient of proportionality between the Joule power P of the dc current released in the sample and the electron temperature increase ΔT (for small electron overheating $\Delta T << T$).

wave number of thermal phonons, l is the electron mean free path):

$$\tau_{e-ph} = 7.6 \cdot 10^{-4} \frac{M}{N_A} \frac{\rho}{R_Q} \frac{p_F^3 u_t^5}{(k_B T)^4 v_F} \quad . \qquad (4)$$

Here N_A is the Avogadro constant, $R_Q = \hbar/e^2 = 4.1$ kΩ is the quantum resistance, u_t is the transverse sound velocity, M is the molar mass, and p_F and v_F are the Fermi momentum and velocity, correspondingly. Equation (4) has been derived from the expression $\tau_{e\text{-}ph}(T)$ for electron scattering from transverse phonons [11]. The transverse phonons strongly dominate in electron-phonon interactions in the dirty limit. The condition of the dirty limit, $q_T l << 1$, is satisfied for our highly disordered Hf films at $T \leq 50$ K. It has been also assumed in Eq. (4) that the electron scatterers (impurities, defects, etc.) are completely dragged by phonons [12]. Finally, we took into account the energy averaging of $\tau_{e\text{-}ph}$ over the Fermi distribution of electrons (see, e.g., [13]).

Using parameters of bulk Hf ($M = 178.5$ g/mol, $u_t = 1.97 \cdot 10^5$cm/s, $p_F = 1.2 \cdot 10^{-19}$ g·cm/s, $v_F = 1.6 \cdot 10^8$cm/s), and the resistivity of the films studied ($\rho = 0.1$ mΩ·cm), we find $\tau_{e\text{-}ph}(T) = 4.8 \cdot 10^{-8}$ s·[1K/T]^4 (the solid line in Fig. 7). Below $T \sim 0.5$ K, the

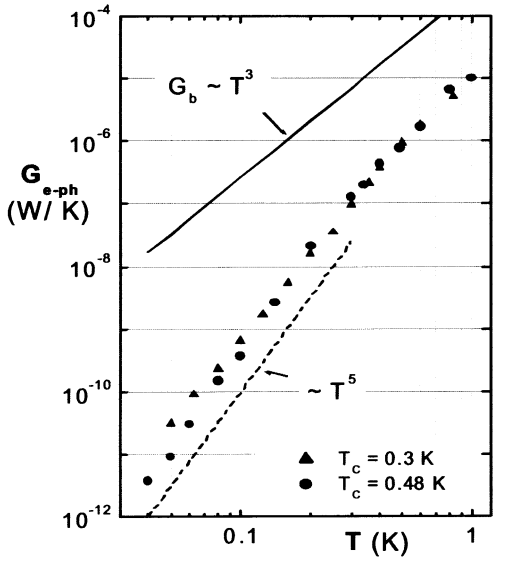

Fig. 6. Temperature dependences of the thermal conductivity $G_{e\text{-}ph}$ for 250 Å-thick Hf meanders with the total area 0.5 mm^2, deposited on sapphire substrates. The solid line is the theoretical estimate for the thermal conductivity G_b of the metal-sapphire interface [7].

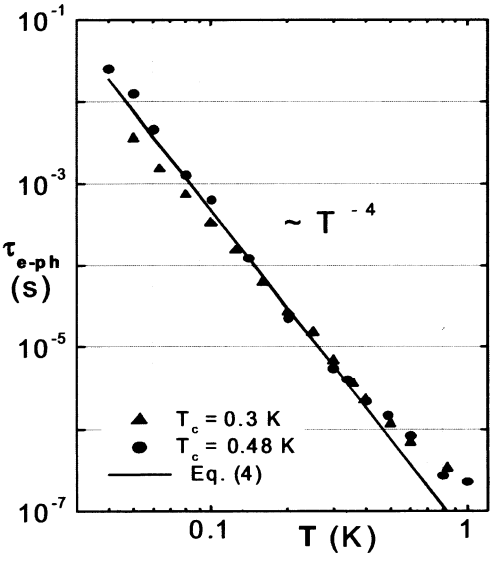

Fig. 7. The electron cooling time $\tau_{e\text{-}ph}(T)$ for 250 Å-thick Hf films with the resistivity $\rho = 0.1$ mΩ·cm. For the other three Hf films with similar ρ, $\tau_{e\text{-}ph}$ was in the range 4 – 9 ms at $T = 40$ mK. The solid line is the dependence $\tau_{e\text{-}ph}(T)$ (Eq. 4) calculated for Hf with $\rho = 0.1$ mΩ·cm.

agreement between the experimental data and Eq. 4 is very impressive (note that this comparison does not involve *any* fitting parameters). At higher temperatures, the dependence $\tau_{e\text{-}ph}(T)$ becomes slower than that predicted by Eq. 4.

Two important conclusions can be drawn from these experiments. Firstly, the experimental values of $\tau_{e\text{-}ph}$ are sufficiently large to ensure record sensitivity of HEDDs at temperatures $T < 0.3$ K. In fact, the value $\tau_{e\text{-}ph} = 25$ ms measured at $T = 40$ mK is, to our knowledge, the largest value of $\tau_{e\text{-}ph}$ ever observed in metals. Secondly, the theory [11,12] provides a reliable estimate of $\tau_{e\text{-}ph}$ in disordered metal films at millikelvin temperatures.

Performance of a micron-size Hf HEDD

Let us estimate the performance of HEDDs fabricated from a disordered hafnium film. Our measurements show that $\tau_{e\text{-}ph}$ in these films can be as large as ~ 0.7 ms at $T = 0.1$ (see Fig. 7). For a HEDD with the sensor dimensions 1x1x0.02 μm^3, we performed a computer modeling of basic characteristics. The modeling procedure, which is similar for all non-equilibrium hot-electron devices, is based on the heat balance equation:

$$\frac{\gamma V}{6\tau_{e-ph}(1K)}\left(T_e^6 - T^6\right) = V_b^2 / R(T_e) \ , \qquad (5)$$

where V_b is the voltage across the device. The temperature-dependent device resistance, $R(T_e)$, was modeled as a smooth function with $dR/dT_{|T=T_c} = R_n/\delta T_c$, where R_n is the device normal resistance and δT_c is the width of the superconducting transition. The modeling was performed for $T_c = 0.3$ K and $T_c = 0.1$ K, assuming that one can fabricate Hf films with different critical temperatures by varying the film deposition conditions. The bath temperature was assumed to be equal $T_c/2$ in both cases.

The fundamental sensitivity limit for the detector is set by fluctuations of the electron temperature (Eq. 2). Besides that, the Johnson-Nyquist noise and amplifier contribution should be considered. The two latter contributions can be minimized, if the responsivity of the detector is sufficiently high. Voltage biasing of superconducting bolometers [14] helps to obtain high current responsivity and, at the same time, to reduce significantly the time constant without affecting the sensitivity. This occurs due to a strong electro-thermal feedback in the bolometer bias circuit. The responsivity $S_I = -(1/V_b)C/(C+1)$ can be expressed in terms of the self-heating parameter $C = (V_b/R)^2(dR/dT)/G_{e\text{-}ph}$, also known as the ETF loop gain. The latter parameter is always positive in superconducting bolometers because $dR/dT > 0$. In order to take advantage of the ETF effect, the bolometer should be driven by the bias current at $T < T_c$ to the state with negative differential resistance (this bias current is very close to the critical current). Relationship between C and the differential resistance dV_b/dI [15]

$$C = \left(dV_b/dI - R\right)/\left(dV_b/dI + R\right) \qquad (6)$$

shows that the self-heating parameter can be very large if $-dV_b/dI \sim R$. Under these conditions, the time constant of the bolometer is reduced by a factor $(C+1)$.

Figure 8 shows the results of modeling. The SQUID amplifier contribution was estimated as $NEP_{SQUID} = i_n/S_I$ (for modern dc SQUID amplifiers, the typical noise $i_n \sim 1$ pA/√Hz [16]). The Johnson-Nyquist noise contribution is given by $NEP_J = (4k_B T_e V_b^2/R)^{1/2}/C$ [17]. This contribution can be significantly reduced due to a large value of parameter C. This occurs at low bias voltages, where fluctuations of the electron temperature dominate and the NEP is minimal. The device dc resistance is small

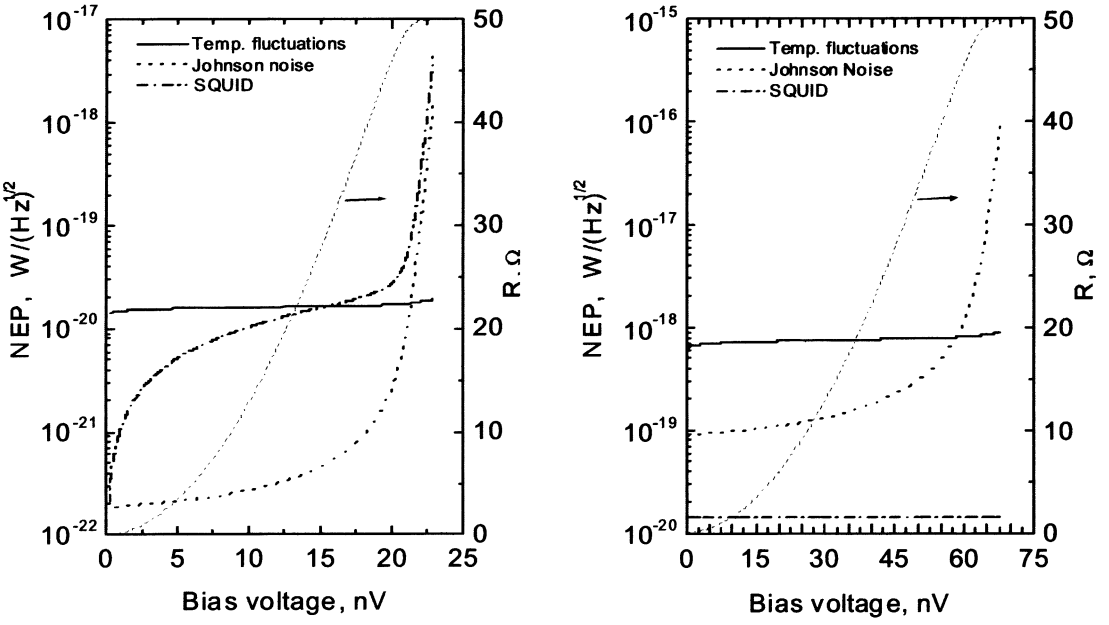

Fig. 8. Contributions of different noise sources to the total noise of the HEDD. Left panel: $T_c = 0.1$ K, right panel: $T_c = 0.3$ K. The detector should operate at low bias voltages to allow for a larger value of the self-heating parameter and a lower value of the device resistance. In this case, the temperature fluctuation noise dominates and the NEP is minimal.

(≤ 1 Ω), which simplifies matching to a SQUID amplifier. At the same time, the device impedance at the signal frequency is high (50-100 Ω), since the photon energy is much greater than the suppressed superconducting gap in the microbridge. At 0.1 K, the self-heating parameter can be as large as 30. In this case, the device time constant will be $\tau = \tau_{e\text{-}ph}/(C+1) \sim 20$ μs, and the energy resolution $NEP\sqrt{\tau}$ will be 7×10^{-23} J, which corresponds to a ~ 100 GHz photon energy. This sensitivity exceeds by far the performance estimated for the other types of direct detectors [10,18]. Even at $T = 0.3$ K, the detector noise performance, $NEP = 7\times10^{-19}$ W/√Hz , is better than that for the state-

of-the-art bolometers operating at or below 0.1 K. The time constant at this temperature is expected to be ~ 7 μs.

Acknowledgment.

We thank O. Harnack for fabrication of photomasks. This research was supported by the Caltech President's Fund. The work at the Jet Propulsion Laboratory, California Institute of Technology, was supported by NASA.

REFERENCES

1. B. S. Karasik, W. R. McGrath, H. G. LeDuc, and M. E. Gershenson, "A Hot-Electron Direct Detector for Radioastronomy", *Supercond. Sci. Technol.* **12**, 745 (1999).
2. M. Shao *et al.*, "Space-based interferometric telescopes for the far infrared", presented at the *SPIE Int. Symp. on Astronomical Telescopes and Instrumentation 2000.*
3. J. C. Mather, S. H. Moseley, Jr., D. Leisawitz, E. Dwek, P. Hacking, M. Harwit, L. G. Mundy, R. F. Mushotzky, D. Neufeld, D. Spergel, and E. L. Wright, "The Submillimeter Frontier: a Space Science Imperative", *http://xxx.lanl.gov/astro-ph/9812454.*
4. J. J. Bock, J. Glenn, S. M. Grannan, K. D. Irwin, A. E. Lange, H. G. LeDuc, and A. D. Turner, "Silicon nitride micromash bolometer arrays for SPIRE", *Proc. SPIE* **3357**, 297 (1998).
5 J. M Gildemeister, A. T. Lee, and P. L. Richards, "A fully lithographed voltage-biased superconducting spiderweb bolometer", *Appl. Phys. Lett.* **74**, 868 (1999).
6. B. S. Karasik, W. R. McGrath, M. E. Gershenson, and A. V. Sergeev, "Photon-noise limited direct detector based on disorder controlled electron heating", *J. Appl. Phys.*, **87**, N10 (2000).
7. E. T. Swartz and R. O. Pöhl, "Thermal boundary resistance", *Rev. Mod. Phys.* **61**, 605 (1989).
8. E. M. Gershenzon, M. E. Gershenzon, G. N. Goltsman, A. D. Semenov, and A. V. Sergeev, "On the limiting characteristics of high-speed superconducting bolometers", *Sov. Phys. - J. Tech. Phys.* **34**, 195 (1989).
9. A. Sergeev and M. Reizer, "Photoresponse mechanisms of thin superconducting films and superconducting detectors", *Int. J. Mod. Phys.* **10**, 635 (1996).
10. M Nahum and J.M. Martinis, "Ultrasensitive-hot-electron microbolometers", *Appl. Phys. Lett.* **63**, 3075, (1993).
11. M. Yu. Reizer and A. V. Sergeev, *Sov. Phys.- JETP* **63**, 616 (1986); J. Rammer and A. Schmid, *Phys. Rev.* B **34**, 1352 (1987).
12. A. Sergeev and V. Mitin, "Electron -phonon interaction in disordered conductors: Static and vibrating scattering potentials", *Phys. Rev. B.* **61**, 6041 (2000).

13. K. S. Il'in, N. G. Ptitsina, A. V. Sergeev, G. N. Goltsman, E. M. Gershenzon, B. S. Karasik, E. V. Pechen, and S. I. Krasnosvobodtsev, "Interrelation of resistivity and inelastic electron-phonon scattering rate in impure NbC films", *Phys. Rev.* B **57**, 15623 (1998).
14. K. D. Irwin, "An application of electrothermal feedback for high resolution cryogenic particle detection", *Appl. Phys. Lett.* **66**, 1998 (1995); A. T. Lee, P. L. Richards, S. W. Nam, B. Cabrera, and K. D. Irwin, "A superconducting bolometer with strong electrothermal feedback", *Appl. Phys. Lett.* **69**, 1801 (1996).
15. H. Ekström, B.S. Karasik, E.L. Kollberg, and S. Yngvesson, "Conversion gain and noise of niobium supercondcuting hot-electron-mixers", IEEE Trans. on Microwave Theory and Technique **43**, 938 (1995).
16. M. Frericks, H.F.C. Hoevers, P.de Groene, W.A. Mels, and P.A.J. de Korte, "Trade-of study of the SQUID read-out for hot-electron micro calorimetry", *J. Phys. IV France* **8**, Pr3-233 (1998); V. Polushkin, D. Glowacka, R. Hart, and J.M. Lumley, "Broadband SQUID amplifiers for photonic applications", *IEEE Trans. Appl. Supercond.* **9**, 4436 (1999).
17. J.C. Mather, "Bolometer noise: nonequilibrium theory", *Appl. Opt.* **21**, 1125 (1982).
18. A.N. Vystavkin, D.V. Shouvaev, L.S. Kuzmin, M.A. Tarasov, E. Andrestedt, M. Wilander, and T. Claeson, "Normal-metal hot-electron bolometer with Andreev reflection from superconductor boundaries", *Sov. Phys.- JETP* **88**, 598 (1999).